Available online at www.sciencedirect.com

ScienceDirect

ELSEVIER

International Journal of Heat and Mass Transfer 50 (2007) 1715–1722

International Journal of HEAT and MASS TRANSFER

www.elsevier.com/locate/ijhmt

Modeling of a conceptual self-sustained liquid fuel vaporization–combustion system with radiative output using inert porous media

Tarun K. Kayal *, Mithiles Chakravarty

Chemical Engineering Section, Central Glass and Ceramic Research Institute, Kolkata 700 032, India

Received 24 June 2005; received in revised form 9 October 2006
Available online 2 January 2007

Abstract

The present model is based on a combined self-sustained liquid fuel vaporization–combustion system, where the liquid fuel vaporization occurs on a wetted wall plate with energy transferred through the plate from the combustion of vaporized oil. The vaporization energy has been derived through the radiative interaction of the vaporizing plate and an upstream end surface of the porous medium. The inert porous medium, used in the flow passage of combustion gas, is allowed to emit and absorb radiant energy. The radiative heat flux equations for the porous medium have been derived using the two-flux gray approximation. The work analyzes the effect of emissivities of vaporizing plate and porous medium, the optical thickness of medium and equivalence ratio on the kerosene vaporization rate, combustion temperature and radiative output of the system. Combination of low and high emissivities of vaporizing plate and porous medium respectively with low optical thickness of medium makes the system operable over a wide range of power. The study covers the data concerning the design and operating characteristics of a practical system.

Keywords: Liquid fuel combustion; Inert porous medium; Heat transfer; Radiation; Modeling

1. Introduction

Porous media gas burners have been used in various thermal applications [1,2] due to their several advantages over conventional burners. The advantages are higher thermal efficiency, high power density (compact), better flame stability and low emission of CO and NO_X. Many analytical and experimental studies have been performed to analyze the combustion characteristics of porous medium burner for premixed gaseous fuel–air system [3–7]. But only a few studies have been reported for combustion of liquid fuel using porous medium. Kaplan and Hall [8] and Durst et al. [9] used premixed fuel oil sprayed droplets in air in place of gaseous fuel–air mixture and studied the effect of various parameters on stabilized combustion inside porous ceramic matrix. Martynenko et al. [10] investigated, by numerical simulation, self-sustaining combustion of a gaseous mixture in inert porous medium with prior vaporization of fuel droplets. The collision of the fuel oil droplets on the porous matrix and effect of heat transfer coefficient between liquid and solid on the porous matrix superheat were incorporated in the heat transfer analysis. Kayal and Chakravarty [11] investigated, by numerical analysis, the combustion of fuel oil droplets suspended in air inside an inert porous medium where the complete vaporization of fuel oil droplets occurs prior to their entry in the combustion zone inside the medium. The effects of various properties of the medium on the radiative energy output and optimum fuel oil droplet size at the entry, defined as the maximum size for complete vaporization before entering the combustion zone, have been presented. Kayal and Chakravarty [12] have performed a numerical analysis of fuel oil combustion inside an inert porous medium where

---

[*] Corresponding author.
E-mail address: tarun@cgcri.res.in (T.K. Kayal).

0017-9310/$ - see front matter © 2006 Elsevier Ltd. All rights reserved.
doi:10.1016/j.ijheatmasstransfer.2006.10.044

Nomenclature

a	specific area, m^{-1}
b	fraction of area of plate 1 used for fuel oil preheating
c_p	average specific heat, $\mathrm{J\,kg^{-1}\,K^{-1}}$
D_1, D_2, D_3	distances in Fig. 1
E^*	downstream radiative efficiency, $q^*(L)/q'$
E'	emissivity of plate 1
E''	emissivity of porous medium
f	equivalence ratio
h	heat transfer coefficient, $\mathrm{W\,m^{-2}\,K^{-1}}$
h_1	heat transfer coefficient between plate 1 and fuel oil in preheating section of the plate, $\mathrm{W\,m^{-2}\,K^{-1}}$
h_2	heat transfer coefficient between plate 1 and fuel oil in fuel vaporizing section of the plate, $\mathrm{W\,m^{-2}\,K^{-1}}$
i	radiation intensity, $\mathrm{W\,m^{-2}}$
i_b	black body intensity, $\mathrm{W\,m^{-2}}$
k	average thermal conductivity, $\mathrm{W\,m^{-1}\,K^{-1}}$
L	porous layer length, m
L^*	optical length, αL
m	fuel oil flow rate, $\mathrm{kg\,m^{-2}\,s^{-1}}$
M_{av}	average molecular weight, $\mathrm{kg\,mol^{-1}}$
M_1, M_2, M_3	dimensionless quantities as in Eq. (12)
n_f	fuel concentration, $\mathrm{kg\,mol\,m^{-3}}$
n_{O_2}	oxygen concentration, $\mathrm{kg\,mol\,m^{-3}}$
p	pressure, $\mathrm{N\,m^{-2}}$
q	radiative heat flux, $\mathrm{W\,m^{-2}}$
q_v	heat flux for fuel oil vaporization, $\mathrm{W\,m^{-2}}$
q^*	net radiative heat flux, $\mathrm{W\,m^{-2}}$
q'	reaction enthalpy flux, $\mathrm{W\,m^{-2}}$
Q^*	dimensionless reaction enthalpy flux, $q'/(\sigma T_i^4)$
R	universal gas constant, $\mathrm{J\,kg\,mol^{-1}\,K^{-1}}$
s	scattering coefficient of porous medium, m^{-1}
T	temperature, K
T'	combustion temperature, K
T^*	dimensionless gas temperature, $(T_g - T_i)/T_i$
$T^{*\prime}$	dimensionless combustion temperature, $(T' - T_i)/T_i$
u	average gas velocity, $\mathrm{m\,s^{-1}}$
u_L	laminar burning velocity of stoichiometric fuel oil–air mixture, $\mathrm{m\,s^{-1}}$
V^*	dimensionless burning velocity, $u_2 u_L^{-1}$
x	axial coordinate, m
X	dimensionless axial coordinate, $x\,L^{-1}$
$\tilde{y}$	mass fraction of gaseous product

Greek symbols

α	absorption coefficient of porous medium, m^{-1}
ϕ	porosity
ρ	average density, $\mathrm{kg\,m^{-3}}$
λ	latent heat of vaporization of fuel oil, $\mathrm{kJ\,kg^{-1}}$
σ	Stephen–Boltzmann constant, $\mathrm{W\,m^{-2}\,k^{-4}}$
Δ	difference

Superscripts

$+$	forward direction
$-$	backward direction

Subscripts

a	air
b	boiling point
g	gas
gs	between gas and solid
i	inlet
s	solid
l	liquid
L	at $x = L$
v	vapor
1, 2, 3	interfacial planes

fuel oil flows through the porous medium under gravity wetting its solid wall with concurrent movement of liquid fuel and air under steady state conditions. Effects of various properties of porous medium and operating parameters on radiative energy output have been presented.

Tseng and Howell [13] have conducted experimental and numerical studies of liquid heptane droplet vaporization and combustion of gaseous mixture inside the inert porous medium made of zirconia. The flashback and blow-off limits of the combustion within the porous structure were determined. It was concluded that the smaller droplets size (<25 μm) of heptane could be evaporated in the low temperature region before the flame front.

Takami et al. [14] studied the performance of combustion of kerosene oil when it was added dropwise at the top surface of the porous ceramic plate and ignited on the bottom surface. Jugjai et al. [15] developed a porous medium burner where kerosene oil was supplied dropwise to the top surface of the burner and swirling combustion air was supplied at the lower side of the medium where an opposite flow mixing of oil vapor and air occurred. Combustion occurred inside the medium. Jugjai and Polmart [16] used a set up containing porous medium and packed bed with air mixing chamber in between them. Kerosene was added dropwise to the top of the ceramic matrix. Kerosene vapor, formed during the passage of fuel oil through the matrix, was mixed with air in the combustion chamber and the combustion gas finally passes through the packed bed to convert a portion of gas sensitive heat to radiant energy. Temperature profiles for both axial and radial position of the set up were measured and analyzed. Fuse et al. [17] used a porous ceramic plate as the fuel evaporating element where the radiant energy from the flame and furnace walls penetrate through the large pores of the ceramic plate to the downstream end and vaporize the kerosene oil in a container. This way the radiant energy was utilized effectively to sustain oil vaporization. Here the sustenance of fuel oil vaporization was primarily controlled by the optical thickness of the ceramic plate.

It is seen that recent works are mainly aimed at utilizing a portion of fuel oil combustion enthalpy for fuel oil evaporation prior to its combustion. Then the hot combustion gas is finally passed through the porous medium for efficient conversion of gas sensible heat to radiant energy at the downstream end.

In the present study, all the above operations and processes are incorporated in a system where the fuel oil vaporization occurs on a wetted wall plate. The heat released from the combustion process is used to preheat and vaporize the fuel by heating the plate. Heat transfer from the combustion products to the porous matrix generates radiative output from the downstream end of the burner.

2. Mathematical analysis

2.1. Analytical model

The schematic diagram representing two-dimensional model under steady state condition is shown in Fig. 1. The system is divided into three regions A, B and C where A and B region are open spaces and C region contains a porous medium. The interfacial planes (1, 2, 3) are perpendicular to x-direction and separating the regions. The vertical plate 1 separates region A and B. The fuel oil ($T_l = T_i$) enters at $x = -D_1$, $y = 0$ and moves from $y = 0$ to $y = D_2$ under gravity in the form of a thin film along the vertical plate 1. During this passage, the liquid fuel is heated from T_i to boiling point T_b and vaporized completely at $y = D_2$. A suitable air ejector sucks the fuel vapour from region A through bottom opening (height $= D_3 - D_2$) of plate 1 to region B. The air ejector is at the bottom of region B at $y = D_3$ between $x = 0$ to $x = -D_1$. This not only prevents the flashback of flame from combustion zone of region B to region A but also uses region B as a well-stirred combustion reactor having high swirl and back mixing of gaseous components for completion of combustion at $T_g = T'$. In region B, the combustion zone is assumed to be in the space between $x = 0$ to $-D_1$ and $y = 0$ to D_2. Heat of vaporization of fuel is transferred from combustion zone at region B to region A through the plate 1. The combustion products move from combustion zone in x-direction in between $y = 0$ to $y = D_2$ through the porous medium in laminar flow in region C and leaves the region at $T_g = T_L$.

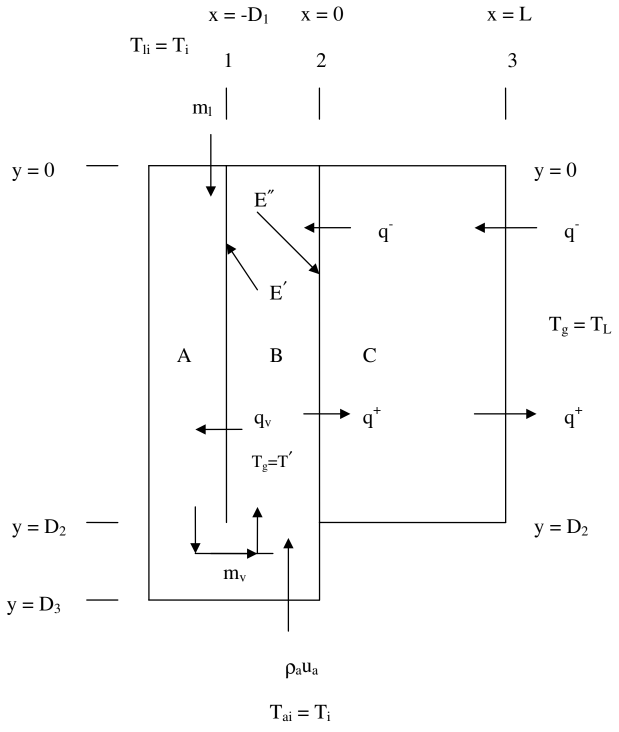

Fig. 1. Schematic diagram of oil combustion system.

Initially region B space is heated through combustion of a fuel gas (methane) in air where both gas and air enter through air port. After sufficient temperature of combustion is reached in region B, the radiative heat becomes sufficient in region B to heat plate 1 for vaporization of fuel oil. Then the fuel gas is switched off. The system becomes self-sustained for vaporization and combustion of fuel oil. The system is insulated and assumed to have no heat loss. The radiative heat fluxes in forward and backward directions in the porous medium are q^+ and q^- respectively. The principal assumptions used in the formation are as follows:

(a) The rate of fuel flow entering region A is optimum such that the fuel oil vaporization is complete just when fuel oil reaches the bottom edge of the plate 1 at $y = D_2$ i.e. $m_l = m_v$.
(b) The temperature along the fuel oil thickness of thin falling film in x-direction on the plate 1 is uniform.
(c) The plate 1 is thermally thin and highly conductive, so that the temperature of the plate is uniform at $T = T_1$ in all directions.
(d) The gases present in the system are non-radiating.
(e) The porous medium in region C is having a high porosity and the gas flow is laminar so that the pressure drop across the medium is negligible.
(f) The porous medium is able to emit and absorb radiation in local thermal equilibrium while radiative scattering effect is ignored.
(g) A one-dimensional radiative propagation occurs in x-direction in the porous medium without any reaction.
(h) Inlet air at $T_{ai} = T_i$ and the oil vapor from region A are thoroughly mixed before the mixture enters the combustion region at $y = D_2$ between $x = 0$ to $x = -D_1$.
(i) The combustion reaction starts and gets completed in the region at constant temperature $T_g = T'$.

(j) Radiative energy exchange in region B occurs between two parallel large surfaces (1 and 2) having equal areas.
(k) The one step global irreversible reaction mechanism between fuel oil vapor and air is considered.

Some of these assumptions are discussed in detail. The assumption (d) is realized as the emissivity of gas is much less than the porous solid medium. The assumption (e) is justified as the usual matrix structure of radiant burner [18] is in the form of ceramic porous open cellular foams of ceramic fiber structure having porosity in the range of 0.95–0.99. Low pressure drop is justified for laminar flow of gas through these highly porous medium. The assumption (f) is justified to cover most of the porous medium such as ceramic foam [5] and porous metallic medium [19]. The assumption (g) is reasonable due to high thermal insulation outside the duct in presence of negligible radial flow. In the assumptions (i) and (k), the one step global reaction rate for combustion of kerosene vapor in air [20] is given by $k_c = 5 \times 10^{11} \exp[-30{,}000/RT_g][n_f]^{0.25}[n_{O_2}]^{1.5}$ g mol/cm^3/s when n_f and n_{O_2} are fuel vapour and oxygen concentration respectively using kerosene ($C_{12}H_{24}$). With reaction temperature of this system assumed at 1500 K and 99% completion of reaction in a well-stirred reactor, the distance d_1 between the interfacial plane 1 and 2 along x-axis in region B is estimated [20] to be about 2.0 cm for reaction enthalpy flux, Q^* as 7.5×10^3. This minimum space for region B is used in the system for completion of combustion reaction.

2.2. Basic equations

Using above assumptions, the continuity equations for species, energy equations for solid, liquid and gas phases are formulated respectively [4,21]. In the vaporizing region A, the heat transfer equations can be divided into fuel oil preheating and vaporizing sections where b is the fraction of area of plate 1 used for fuel oil preheating.

$$\begin{aligned} q\mathrm{v} &= m_l[\lambda + c_{pl}(T_b - T_i)] \\ &= bh_1(T_b - T_i)/\ln[(T_1 - T_i)/(T_1 - T_b)] \\ &\quad + (1-b)h_2(T_1 - T_b) \\ &\text{at} \quad x = -D_1, \quad y = 0 \text{ to } y = D_2 \end{aligned} \tag{1}$$

where h_1 and h_2 are heat transfer coefficient between plate 1 and liquid in fuel oil preheating and vaporizing section respectively; T_1 is the temperature of plate 1.

In region B, radiative energy exchange between plate 1 and surface 2 is as follows

$$[1/(1/E' + 1/E'' - 1)][\sigma T'^4 - \sigma T_1^4] = q_v \tag{2}$$

In region C,

$$\rho c_{pg} u(\partial T_g/\partial x) = k_g(\partial^2 T_g/\partial x^2) - h_{gs}a(T_g - T_s) \tag{3}$$

$$\partial q^*/\partial x = k_s(\partial^2 T_s/\partial x^2) + h_{gs}a(T_g - T_s) \tag{4}$$

$$\text{Equation of state}: \rho = M_{av}p/\mathrm{RT_g} \tag{5}$$

The net radiative heat flux, q^* is related to heat fluxes q^+ and q^- in forward and backward direction as

$$q^* = q^+ - q^- \tag{6}$$

Using two-flux gray radiation approximation [21], the equation of transfer for intensity in each hemisphere is integrated over their respective hemispheres to yield forward and backward intensities i^+, i^- as

$$\partial i^+/2\partial x = -(\alpha + s)i^+ + si^- + \alpha i_b \tag{7}$$

$$\partial i^-/2\partial x = -(\alpha + s)i^+ + si^- + \alpha i_b \tag{8}$$

where i_b is the black body radiation intensity. As each of the intensities over their respective hemisphere is constant under the two-flux model, the Eqs. (7) and (8) are integrated over each hemisphere to yield

$$\partial q^+/2\partial x = -(\alpha + s)q^+ + sq^- + \alpha\sigma T_s^4 \tag{9}$$

$$\partial q^-/2\partial x = -(\alpha + s)q^- + sq^+ + \alpha\sigma T_s^4 \tag{10}$$

Other boundary conditions are

$$\begin{aligned} &x = -D_1, \ y = 0: \quad T_{li} = T_i \\ &x = -D_1, \ y = D_2: \quad m\mathrm{v} = m_l \\ &x = -D_1 \text{ to } 0, \ y = D_3: \quad T_{ai} = T_i \\ &x = -D_1 \text{ to } 0, \ y = 0 \text{ to } D_2: \quad T_g = T', \ \tilde{y} = 1 \\ &x = L, \ y = 0 \text{ to } D_2: \quad T_g = T_L, \ q^- = 0 \end{aligned} \tag{11}$$

These equations are transformed into dimensionless form using following dimensionless quantities:

$$\begin{aligned} &X = x/L, \quad T^* = (T_g - T_i)/T_i, \quad M_1 = \rho u c_{pg}/(\sigma T_i^3), \\ &M_2 = k_s/(\sigma T_i^3 L), \quad M_3 = k_g/(\sigma T_i^3 L), \quad L^* = \alpha L \end{aligned} \tag{12}$$

The energy balance of the reaction in region B is worked out by considering the total reaction heat release rate, sensible enthalpy flux of gas and radiative energy flux at both ends. The overall energy balance is made by equating the total reaction heat release rate to the sum of heat for vaporization of fuel, sensible enthalpy flux and radiative heat loss at downstream end. Heat conductive energy flux at downstream end of porous medium is assumed to be negligible [22].

2.3. Numerical solutions

The governing differential equations with both boundary conditions were numerically integrated using collocation method [23]. In this method, the differential equations are converted to nonlinear system of equations with assumed polynomial profiles for temperature and heat fluxes. These algebraic equations have been solved using computer. Collocation method has been used in solving similar problems reported [11,12].

The computation was carried out using kerosene–air system in ceramic porous membrane. Taking composition of kerosene as $C_{12}H_{24}$, similar to that of $C_{12}H_{26}$ in absence of detailed data of $C_{12}H_{24}$, the properties of $C_{12}H_{26}$ as a function of temperature has been used [20]. The values of

h_1 and h_2 have been estimated for falling liquid film using the ratio of height to width of plate 1 in the range 1–5 [24]. The value of h_{gs} a of the porous medium was estimated by Sathe et al. [4]. The kerosene–air system, laminar burning velocity, u_L for $f = 1$ at 477 K is taken [25] as 0.40 m s^{-1} The base line data are as follows:

$$\begin{aligned}
&T_i = 298\ \text{K}, \quad f = 1.0, \quad L = 0.05\text{m}, \quad \phi = 0.95,\\
&C_{pg} = 1.105\ \text{kJ/kg/K},\\
&T_b = 489\ \text{K}, \quad k_g = 0.078\ \text{W/m/K}, \quad k_s = 0.18\ \text{W/m/K},\\
&h_{gs}a = 2 \times 10^7\ \text{W/m}^3\text{/K},\\
&\alpha = 20\ \text{m}^{-1}, \quad E' = 0.05, \quad E'' = 0.3
\end{aligned}$$

3. Results and discussion

The temperature of gas and solid inside the porous medium in region C coincide due to high value of h_{gs} a imposed [3,5]. In this study, the combustion temperature, T' remains above 1500 K in the range 1500–2240 K. So the assumption (i) of constant combustion temperature, $T^{*\prime}$ is satisfied. In the system, the optical thickness $L^*(=\alpha L)$ can be changed by varying the absorption coefficient of the porous medium, α while L remains same at 0.05 m. Fig. 2 shows the effect of optical thickness of porous medium, L^* on the thermal performance of the system for constant emissivities of plate 1 and porous medium, E' and E'' respectively. The combustion temperature, $T^{*\prime}$ determines the liquid fuel input rate m_l as per the assumption (a) which is elaborated in Eqs. (1) and (2) with boundary conditions at Eq. (11). As $T^{*\prime}$ increases, the fuel input rate m_l increases due to increase in heat transfer rate to the flowing liquid on the plate 1 from the combustion zone at region B. As L^* increases, the reaction temperature $T^{*\prime}$ and burning velocity, V^* increase due to increased radiative energy feedback from the post flame region to reaction zone. Similar observations have been made earlier [3]. In other words, the increase in L^* leads to increase in fuel input rate, m_l and reaction enthalpy flux, Q^*. The effect of L^* on Q^* is significant as Q^* increases by nearly 450% with only 50% increase in L^*. This sharp increase in Q^* also leads to the decrease in radiative output efficiency E^* with increase in L^*. It can be concluded that the optical thickness of the porous medium affects the fuel input rate significantly. Low values of absorption coefficient have been obtained using low pore density of medium [16] and will fit into the range of L^* used in this paper. From the point of view of radiative energy usage to heat the load at downstream end, it is desired to use low optical thickness of porous medium.

Fig. 3 shows the effect of emissivity of the porous medium, E'' on the performance of the system for constant emissivity, E' of plate 1 and optical thickness, L^* of the medium. Emissivity of the porous medium affects the radiative energy exchange between plate1 and surface 2 of porous medium as indicated in Eq. (2). As E'' increases, more radiative energy flux is transferred for fuel oil vaporization resulting in the increase of fuel input rate, m_l, and combustion enthalpy flux, Q^*. This ultimately increases the combustion temperature, $T^{*\prime}$ and burning velocity, V^*. It is seen that effect of E'' is similar to that of optical thickness, L^* of the porous medium. The thermal performance of the system is only affected by the change in radiative character

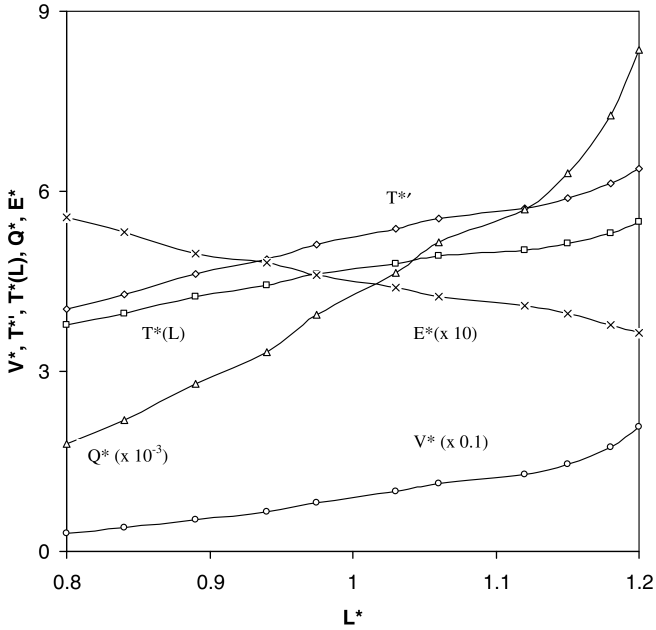

Fig. 2. Effect of optical thickness of porous medium on combustion and exit gas temperature, burning velocity, reaction heat flux and downstream radiative efficiency at $E' = 0.05$, $E'' = 0.3$.

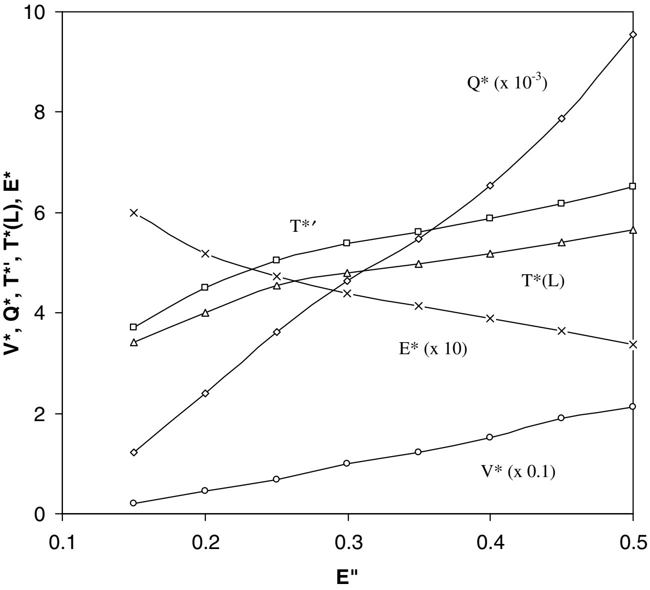

Fig. 3. Effect of emissivity of porous medium on reaction heat flux, combustion and exit gas temperature, burning velocity and radiative output for $E' = 0.05$ and $L^* = 1.03$.

of surface 2 of the porous medium. So surface coating of suitable emissivity, E'' on the surface 2 of the porous medium is only required to affect the thermal performance of the system instead of changing the emissivity of the entire porous medium to E''. The porous ceramic medium is usually made of Al_2O_3 or ZrO_2 in the form of foam or fibers. At 2000 K, the values of emissivity, E'' for Al_2O_3 and ZrO_2 are 0.28 and 0.31 respectively [2]. SiC, which is having high emissivity [2], may be suitably used in coating the surface 2 of the porous medium in wide range of E'' for the system.

The effect of either of emissivity, E' of plate 1 or emissivity, (E'') of porous medium is similar on the thermal performance of the system. So the increase in E' will increase the combustion temperature, $T^{*\prime}$ as shown in Fig. 4. Whereas the effect of decrease of optical thickness, L^* on the system is to decrease the combustion temperature, T^*. So to maintain constant $T^{*\prime}$, the increase in emissivity, E' of plate 1 is to be coupled with decrease in the optical thickness, L^* of the porous medium. Fig. 4 shows the thermal performance of the system at constant combustion temperature $T^{*\prime} = 6.215$ (i.e. $T' = 2150$ K). For $E' < 0.06$, L^* decreases sharply with increase in E'. For $E' > 0.06$, the decrease of L^* is not significant with increase in E'. With increase in E', the fuel input rate, m_1 and reaction enthalpy flux, Q^* increase due to increase in the radiative energy exchange rate between surface 2 of porous medium and plate 1 as indicated in Eq. (2). The effect of E' or E'' is interchangeable in Eq. (2). The effects of E'' and E' on different variables are similar as shown in Fig. 3 and 4. The change of emissivity, E' of plate 1 in the low range (0.045–0.12) is practical because the values of emisivity, E' of gold plating on steel [26], silver, oxidized zinc and aluminium [27] at 489 K are nearly 0.05, 0.02, 0.11 and 0.113 respectively. These metallic materials may be used for construction of plate 1.

It is seen from Figs. 2–4 that the combination of low value of E' and high value of E'' have been used keeping in view the practical aspect of material of construction of the system. The equations could not be solved with combinations of high values both E' and E''. In practical terms, this combination will lead to high oil vaporization rate and accordingly high air flow rate when the combustion energy will exit the porous medium in form of gas sensible heat without its conversion by the porous medium to radiative heat flux.

Fig. 5 shows the effect of equivalence ratio, f on the performance of the system at constant values of emissivities E', E'' and optical thickness of medium, L^*. With increase in f, all the variables increase almost linearly above $f = 0.6$.

Fuse et al. [17] used the radiative energy flux of a porous ceramic plate at the downsream end in vaporizing kerosene from a container while the source of radiative energy to the plate was the combustion flame, burnt gas and furnace walls. In the experiment, 10 porous plates of total area 0.015 m^2 and optical thickness 0.54 were used. At the stabilized combustion with power input 51 kW i.e. 3.4×10^6 W m^{-2}, average equivalence ratio 0.6 and flame temperature in the range 1500–1600 K, the vaporizing energy as the radiative energy flux from the ceramic plate is estimated to be 6.9×10^4 W m^{-2}. This energy flux is only 2.03% of the total power input. In the present investigation (Fig. 5), with power input as 1.18×10^6 W m^{-2} at equivalence ratio 0.6 and flame temperature 1650 K, the combustion energy has been utilized in supporting both fuel oil vaporization energy 1.97×10^4 W m^{-2} and downstream

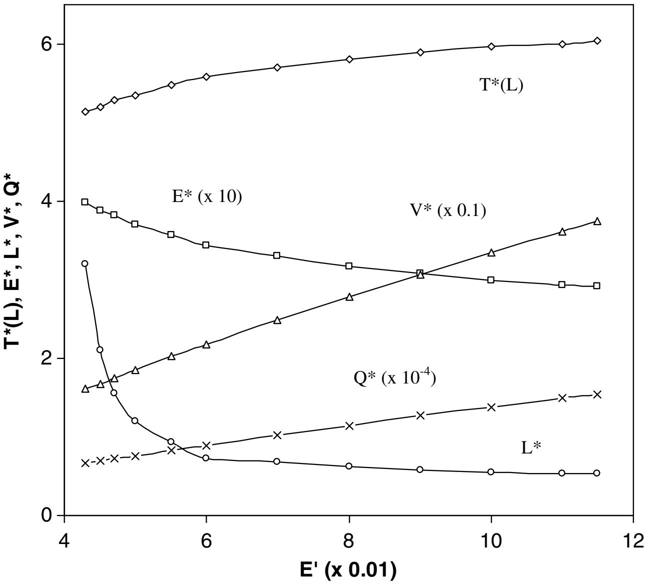

Fig. 4. Effect of emissivity of vaporizing plate on exit gas temperature, burning velocity, reaction heat flux and downstream radiative output with varying combination of optical thickness of medium to maintain $T^{*\prime} = 6.215$ for $E'' = 0.3$.

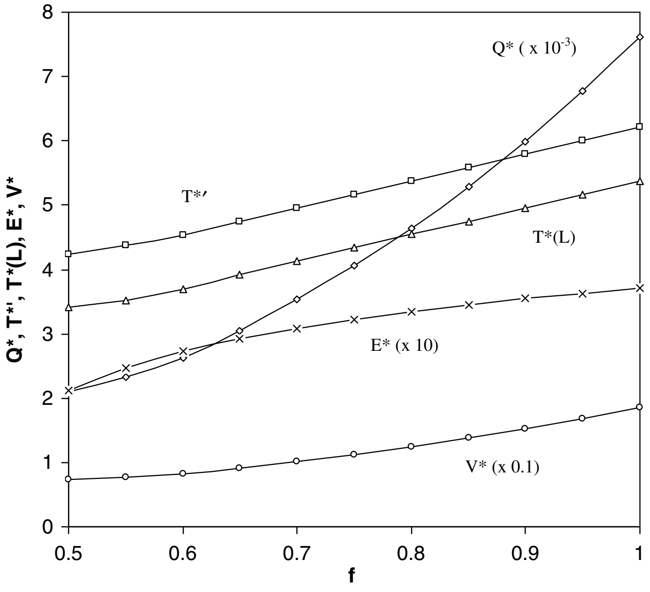

Fig. 5. Effect of equivalence ratio on reaction heat flux, combustion and exit temperature of gas, burning velocity and downstream radiative output for $E' = 0.05$, $E'' = 0.3$ and $L^* = 1.2$.

radiative energy output $3.22 \times 10^5\ \mathrm{W\,m^{-2}}$ using porous medium of optical thickness 1.2. These energy usages are 1.68% and 27.38% of the total power input respectively.

While comparing the data of Fuse with that of the present investigation (Fig. 5), it is seen that in both cases, the temperature of flame and optical thickness of porous medium are of similar order and the vaporizing energy has been derived from the combustion energy. But in the present investigation, an additional radiative energy output is available which may be due to the design of the set up. In Fuse's experiment, the radiative energy from the flame and burnt gas flowing over one face of the porous plate penetrated in perpendicular direction along the thickness of the plate due to its large pore size and low optical thickness. The amount of radiative energy flux from the other end of the plate was small but sufficient to vaporize the fuel oil from container. In the present investigation, the required vaporization energy is first transferred from combustion flame and gas through indirect heating. Then the hot gases passes through the porous medium to convert a portion of sensible heat of gas to radiant energy flux at downstream end. The value of radiant energy flux is large in comparison to that of vaporization energy.

4. Conclusion

A two-dimensional model has been developed based on a system where the liquid fuel is vaporized through indirect heat transfer from vaporized fuel combustion zone and the porous medium converts the sensible heat of the combustion gas to downstream radiative heat flux. The system has been analyzed in operable power range 2.97×10^5–$4.27 \times 10^6\ \mathrm{W\,m^{-2}}$. Following are the conclusions in the present investigation:

1. The material characteristics of the system i.e emissivities of the vaporizing plate and porous medium as well as the optical thickness of the porous medium affect the fuel input rate i.e. power input. Out of them, the effect of optical thickness of medium on the power input is most significant as the power input increases 450% with only 50% increase in optical thickness of media.
2. Combination of low and high emissivities of vaporizing plate and porous medium respectively with low optical thickness of porous medium makes the system operable over a wide range of power inputs.

Efforts may be made to increase the fuel input rate by increasing the evaporating surface area and heat transfer coefficients of liquid flow on the evaporating plate. Addition of fins type extended surface on the plate will serve these purposes.

Acknowledgement

The authors express their sincere gratitude to Dr. H.S. Maiti, Director, CGCRI for his keen interest and encouragement in this work under the Institute project and kind permission to publish this paper.

References

[1] R. Echigo, Effective energy conversion method between gas enthalpy and thermal radiation and application to industrial furnaces, in: Seventh International Heat Transfer Conference, München, vol. 6, 1982, pp. 361–366.

[2] S. Mößbauer, O. Pickenäcker, K. Pickenäcker, D. Trimis, Application of the porous burner technology in energy and heat engineering, in: Fifth International Conference on Technologies and Combustion for a Clean Environment (Clean Air V), Lisbon, Portugal, 1999, pp. 12–15.

[3] Y. Yoshizawa, K. Sasaki, R. Echigo, Analytical study of the structure of radiation controlled flame, Int. J. Heat Mass Transfer 31 (1998) 311–319.

[4] S.B. Sathe, R.E. Peck, T.W. Tong, Flame stabilization and multimode heat transfer in inert porous media: a numerical study, Combust. Sci. Technol. 70 (1990) 73.

[5] P.F. Hsu, J.R. Howell, R.D. Mathews, A numerical investigation of premixed combustion within porous inert media, J. Heat Transfer Trans. ASME 115 (1993) 744–750.

[6] J.R. Howell, M.J. Hall, J.L. Ellzey, Combustion of hydrocarbon fuels within porous inert media, Prog. Energy Combust. Sci. 22 (1996) 121–145.

[7] A.J. Barra, J.L. Ellzey, Heat recirculation and heat transfer in porous burners, Combust. Flame 137 (1–2) (2004) 230.

[8] M. Kapalan, M.J. Hall, The combustion of liquid fuels within a porous media radiant burner, Exp. Therm. Fluid Sci. 11 (1) (1995) 13–20.

[9] F. Durst, M. Keppler, M. Weclas, Air-assisted nozzle applied to very compact, ultra-low emission porous medium oil burner, Third Workshop (Spray 97), Lampoldshausen, 1997.

[10] V.V. Martynenco, R. Echigo, H. Yoshida, Mathematical model of self-sustaining combustion in inert porous medium with phase change under complex heat transfer, Int. J. Heat Mass Transfer 41 (1) (1998) 117.

[11] T.K. Kayal, M. Chakravarty, Combustion of liquid fuel inside inert porous media, Int. J. Heat Mass Transfer 48 (2) (2005) 331–339.

[12] T.K. Kayal, M. Chakravarty, Modeling of trickle flow liquid fuel combustion in inert porous medium, Int. J. Heat Mass Transfer 49 (5–6) (2006) 975–983.

[13] C.-J. Tseng, J.R. Howell, Combustion of liquid fuels in porous medium burner, Combust. Sci. Technol. 112 (1996) 141–161.

[14] H. Takami, T. Sujuki, Y. Itaya, M. Hasatani, Performance of flammability of kerosene and NO_X emission in the porous burner, Fuel 77 (3) (1998) 165–171.

[15] S. Jugjai, N. Wongpanit, T. Laoketkan, S. Nonkkaew, The combustion of liquid fuels using a porous medium, Exp. Therm. Fluid Sci. 26 (1) (2002) 15.

[16] S. Jugjai, N. Polmart, Enhancement of evaporation and combustion of liquid fuels through porous media, Exp. Therm. Fluid Sci. 27 (8) (2003) 901–909.

[17] T. Fuse, Y. Araki, N. Kobayashi, M. Hasatani, Combustion characteristics in oil-vaporizing sustained by radiant heat flux enhanced with higher porous ceramics, Fuel 82 (11) (2003) 1411–1417.

[18] D. Trimis, F. Durst, O. Pickenäcker, K. Pickenäcker, Porous medium combustor versus combustion systems with free flames, in: Second International Symposium on Heat Transfer Enhancement and Energy Conversion, Guangzhou, China, 1997.

[19] H. Yoshida, J.H. Yun, R. Echigo, T. Tomimura, Transient characteristics of combined conduction, convection, and radiation heat transfer in porous media, Int. J. Heat Mass Transfer 33 (5) (1990) 847.

[20] G.L. Borman, K.W. Ragland, Combustion Engineering, McGraw-Hill, New York, 1998, pp. 374, 570.

[21] S.W. Baek, The premixed flame in a radiatively active medium, Combust. Sci. Technol. 64 (1989) 277–287.

[22] R. Echigo, Y. Yoshizawa, K. Hanamura, T. Tomimura, Analytical and experimental studies on radiative propagation in porous media with internal heat generation, in: Eighth International Heat Transfer Conference, Sanfransisco, vol. 2, 1986, pp. 827–832.

[23] P. Razeloes, Methods of obtaining approximate solutions, in: W.M. Rohsenow, J.P. Hartnett (Eds.), Handbook of Heat Transfer, McGraw-Hill, New York, 1973, pp. 4–72.

[24] S.M. Yih, Modeling heat and mass transport in falling liquid film, in: N.P. Cheremisinoff (Ed.), Handbook of Heat and Transfer Mass Transfer and Reactor Design, vol. 2, Gulf Publishing Co, Houston, Texas, 1986, p. 124.

[25] M.W. Thring, The Science of Flames and Furnaces, Chapman and Hall, London, 1962.

[26] W.D. Wood, H.W. Deem, D.F. Lucks, High temperature materials No. 3, Thermal Radiative Properties, Plenum Press, New York, 1968, pp. 382.

[27] E.W. Washburn (Ed.), International Critical Tables, vol. V, McGraw-Hill, New York, 1929, p. 244.